Proceedings of the 2012 IEEE 12th International Conference on Bioinformatics & Bioengineering (BIBE), Larnaca, Cyprus, 11-13 November 2012

Image Guided Mechanically Scanned and Co-registered Localized Optical and MR Spectroscopies

Ahmet E. Sonmez[1], Andrew G. Webb[2] and Nikolaos V. Tsekos[1]
[1]Medical Robotics Lab, Department of Computer Science at University of Houston, Houston, TX, USA
Email: aesonmez@northamerican.edu, ntsekos@cs.uh.edu
[2]Dept of Radiology, Leiden University Medical Center, Leiden, Netherlands. Email: a.webb@lumc.edu

***Abstract*—Interrogation of tissue with combined molecular methods, such as light-induced fluorescence (LIF) and MR spectroscopy (MRS), may lead to new paradigms in assessing tissue malignancy in situ. The limited tissue penetration (LIF) or low sensitivity (MRS) of those modalities is usually addressed by local placement of the sensor via trans-needle or trans-catheter access. This work introduces a system and methodological approaches for mechanically scanning an area of interest with an MR-compatible manipulator that carries two sensors: an optical fiber for LIF and a miniature RF coil for MRS. Experimental studies on multi-compartment phantoms demonstrated dual-modality scanning and the generation of one-dimensional MRS/LIF scans inherently registered to MRI that was used to guide the scanning.**

Keywords-Localized biosensing, MRI, MR Spectroscopy, LIF, multi-modality, co-registration

I. INTRODUCTION

Continuous advances in molecular and cellular or near-cellular modalities, such as optical- and MR-based technologies, opened new opportunities for assessing the malignancy of tumors *in situ* [1]. However, their eventual translation to clinical practices is associated with several challenges. Among them is the limited tissue penetration: for example in the range of 1-3 mm for near-infrared optical methods. To address this limitation, optical-fiber based probes are used to reach a targeted tissue in vivo via trans-needle or trans-catheter access [2]. Similarly, MR spectroscopy (MRS), a powerful modality for assessing the metabolic profile of tissue *in situ*, has low inherent signal sensitivity. As a result, similar to optical methods, miniature MR sensors (i.e., radiofrequency (RF) coils) are placed very close to the tissue of interest, for example in intra-vascular [3] or endo-urethral [4] MR biosensing. With such locally-deployed sensors (i.e., ones that interrogate only a small local volume) another imaging modality with a much larger sensitive area is needed to guide the placement and scanning of the locally-deployed sensors. Then, tissue scanning is performed along the path of the needle or the catheter by manually or mechanically translating the locally-deployed sensors [2-5].

It has been well documented that multi-modality biosensing is important to collect complementary pathophysiologic information. As a consequence, multi-sensor probes have been developed for collecting data from all the sensors at the same position of tissue for spatial localization and high co-registration accuracy that, in turn, offers a higher diagnostic value [5]. Indeed, "single-scan" multimodality sensing can alleviate data mis-registrations, due to possible tissue dislocation or patient movement between the separate scans, as well as accelerate data collection since the multi-sensor needs to pass only once along its path. (e.g. [5]). Within this context, if MRI is used as the guiding modality, an additional benefit with multi-sensor biosensing is that the sensor(s) can be registered to the coordinate system of the MR scanner. As a consequence, the collected data are inherently registered to the MR images. This, in turn, eliminates the need for registration by post-processing. This concept has been proposed before for performing MRI-guided localized MRS [6]. However, that work did not report multi-modality sensing nor demonstrate the practical outcome of multimodality manipulator-based data co-registration and fusion.

Here, we explore the concept of multi-sensor, *single-scan* sensing introduced previously (e.g. [5, 6]), using a computer-controlled MR-compatible manipulator that carries a "locally-deployed" dual MR and optical sensor (i.e. dual MRS/LIF probe) and scans an area of interest via a minimally invasive access approach. Experimental studies with multi-compartment phantoms demonstrate that the dual MRS/LIF probe can collect one-dimensional spatial distributions of optical and MR spectra that are co-registered to the MR image used for guidance.

II. METHODOLOGY

Fig. 1(a) illustrates the schematic architecture of the optical/MRS biosensing system. It consists of four main components. (1) *Image-guided planning:* Using a large volume coil that surrounds the object, scout MRI is used for selecting the scanning parameters (e.g., position/size of scanned zone(s) and spatial scanning resolution) for optical and MR spectroscopies. (2) *Mechanical scanner with dual-sensor:* An MR-compatible manipulator linearly scans with an attached dual sensor composed of a three-fiber endoscope for emitting and receiving light and a miniature RF coil, anchored at its distal end (or end-effector). (3) *Manipulator-based multi-modality co-registration:* After registering the manipulator to the MR coordinate system, the optical and MRS data are also co-registered as the manipulator scans the area of interest. (4)

Automated scanning: Using a triggering scheme advancement of the manipulator, optical and MRS data collection and registration are all automated.

A. System

The system required integration of hardware and software modules for (i) initial registration of the manipulator to the MR scanner and planning the scanning acquisition via a graphical user interface (GUI), (ii) synchronizing the control of the manipulator, the MR scanner and the optical scanner data collection with on-the fly multimodal registration, (iii) processing MR and optical data, and presenting them on the GUI. The central component of the system is an in-house built "control box" based on a microcontroller (MC9S12DG256, 16-bit microcontroller, Freescale, Austin, TX). Using suitable interfaces on the control box, the microcontroller is connected to the PC via a DE-9 connector (RS-232 connection), to the MR scanner with two co-axial BNC cables, and to the optical spectrometer via a DE-9 connector (TTL connections). It hosts run-time code that performs two tasks. First, based on the acquisition parameters uploaded from the PC (set by the operator), it sends and receives TTL pulses to synchronize the motion of the manipulator with data collection from the MR and optical scanners. Fig. 1(b) illustrates an example of such triggering scheme that is used in the studies presented here. Data are collected with the manipulator static and the motor idle at a particular position. Second, the code controls the motion of the manipulator with a closed loop based on the optical encoder signals from the actuator of the manipulator. Automated control of the manipulator, as well as data co-registration and fusion, are performed in the inherent coordinate system of the MR scanner. This is achieved after an initial registration of the manipulator to the MR coordinate system.

The MR-compatible manipulator has one degree-of-freedom and resembles the kinematic structure of the one reported in [6]. However, compared to that work, our manipulator uses a piezoelectric motor (N-310 NEXACT Piezo-Walk motor, PI, Karlsruhe, Germany) that allows bi-directional scanning. The optical setup consists of a spectrometer (USB 2000+, Ocean Optics, FL) and Light Emitting Diode light source (LED 470 filtered at 450nm, Ocean Optics, FL). The MR scanner is a 4.7-T Varian/Agilent DirectDrive™ MR spectrometer/imager (Agilent Technologies, Santa Clara, CA). We modified the pulse sequences for the collection of registration projections and MR spectra to (i) be initiated (triggered) by the TTL signal from the control box, and (ii) return back to it a TTL pulse after the conclusion of data collection (per the scheme in Fig. 1(b)).

B. Dual MRS/LIF Probe

Fig. 2 shows photographs of the dual modality "side-viewing" optical/MR sensor. The current prototype probe is held in a 1.6-mm outer diameter (OD) and 10cm long quartz cylinder (MBT-015-062-4Q, Friedrich & Dimmock Inc., Millville, NJ) with four bores that are used to align the three optical fibers of the optical sensor and carry the coaxial cable of the MR sensor. The optical sensor is composed of three plastic optical fibers (core/cladding/buffer = 200/220/245 microns, numerical aperture (NA) = 0.22) terminated with 0.5-mm leg size right angle prisms (P-788474-S-RTA002, Bern Optics, MA). One optical fiber is used for light emission (Fig. 2(a)) and the other two for light reception (Fig. 2(b)). The three fibers are 10m long and interface to the optical spectrometer (with the two reception fibers combined via a bifurcation) that is located outside the MR room.

The MR sensor is a 1-mm RF coil that is made from a 0.313mm OD and 12 cm long coaxial cable (50MCX-21, Temp-Flex, South Grafton, MA). To form the 1-mm diameter loop of the coil, we stripped the distal end of the center core of the coaxial cable, wound and soldered it back to its shield. The other end of the coaxial cable is connected to a balanced tuning and matching circuit constructed with non-magnetic variable capacitors (Johanson Manufacturing Co, NJ) for fine tuning

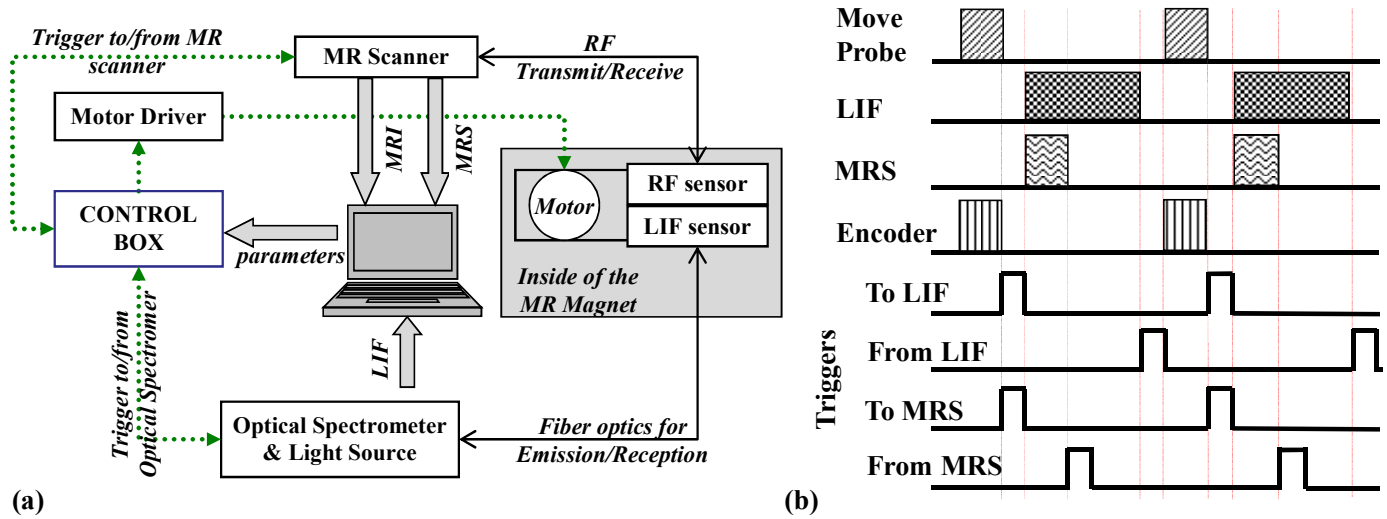

Figure 1. **(a)** Architecture of the MR/LIF mechanically scanned and co-registered bio-sensing system. **(b)** Representative timing diagram of automated operation via triggers.

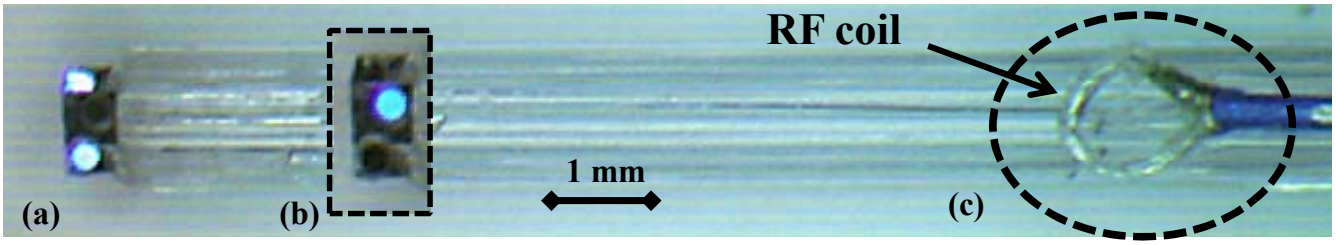

Figure 2. Microscopic photo of the distal end of the optical/MR dual-sensor probe **(a)** The light-receiving optical fibers (shown here illuminated). **(b)** Affixed photo, with the light emission from the illuminating optical fiber at the center **(c)** 1mm diameter miniature RF coil that was placed 1.0 cm away from the optical prisms.

and matching at the proton Larmor frequency of 201.5 MHz (the operating frequency of the 4.7 Tesla MR scanner). The RF coil and the quartz tubing are then attached using optical adhesive (Norland 72, NY). The coil is used as transmit/receive (Tx/Rx) for both MR spectroscopy and registration of the manipulator.

Since the prisms of the optical probe are coated with a thin film of protective aluminum, in order to avoid any distortion of the local magnetic field due to eddy currents or magnetic susceptibility induced artifacts, the center of the RF coil is placed 1.0 cm away from the optical sensor (Fig. 2). The spatial offset between the RF coil and the LIF sensor is accounted for when the optical and MR data were co-registered and fused.

C. Experimental Studies

Although MR and optical data collection are performed with the manipulator idle at a given position, studies were performed to assess whether the motor and optical encoder operation introduce noise to the MR data. In the studies we used a 6.5 % gelatin/water phantom with a volume RF coil around it, and placed the manipulator at its exact position (with the motor 55 cm away from the isocenter of the magnet). Then, we collected MR spectra and scout MRI (30 repetitions) for different states of the motor and optical encoder (EM1, US digital, Vancouver, WA). From these data, we extracted the signal-to-noise ratio (SNR).

To investigate multi-modality scanning of different layers of material (to mimic, for example, the boundary from normal-to-cancerous-to-benign tissue) we used three-compartment gelatin-based phantoms. Each compartment was prepared by adding into the gelatin matrix specific chemicals to be optically and MR, detectable and distinguishable. The composition of the three compartments was. (1) Compartment #1 (comp-1) water based gelatin (with an MRS peak at 4.9 ppm) and the fluorophore fluorescein (518-47-8, Acros, NJ) for LIF. (2) Compartment #2 (comp-2) was oil-based gelatin (with a characteristic MR resonance at 1.4 ppm) and no fluorophore. (3) Compartment #3 (comp-3) was a water-based matrix with choline (with an MR resonance at 3.3 ppm) and two fluorophores, fluorescein and rhodamine-B (83689, Sigma Aldrich, St. Louis, MO), that give characteristic optical spectra [7] when combined. The three compartments were stacked together and a 2.5-mm OD NMR tube (S-2.5-500-, Bruker, Billerica, MA) was inserted orthogonal to their boundaries to create an endoscopic channel for the probe. Fig. 3 shows an MR image of the phantom, zoomed-in to the area of scanning; the oil-based comp-2 exhibits lower signal intensity as compared to the water-based comp-1 and comp-3.

In each study, to perform the initial registration of the manipulator (and thus the LIF/MR sensors) to the MR scanner coordinate system, we collected images using the miniature RF coil as a Tx/Rx fiducial marker (as in [6]). Scout MR images, collected with the volume coil to image the entire phantom, were loaded onto the GUI, and used to set the acquisition parameters. These were: (1) number and length (3.2 cm for presented study) of the scanned region(s) along the channel, (2) specific step size at which each modality was collected (we used 0.5 mm for both LIF and MR), and (3) types and order of acquisitions (as in Fig. 1(b)). The control parameters generated were then uploaded to the control box that automatically runs the synchronized sequence of Fig. 1(b), consisting of the repeating steps of: (1) motion of the sensor to a new position, (2) trigger MR to collect a free induction decay (FID) (flip angle of excitation pulse = 20°; bandwidth = 5000 Hz and number of points = 2048), (3) trigger optical spectrometer for LIF spectra collection of 5s, then repeated at the next position.

The NMR spectra were subject to standard processing including Fourier transformation, phasing [8], baseline correction with a polynomial baseline fitting method

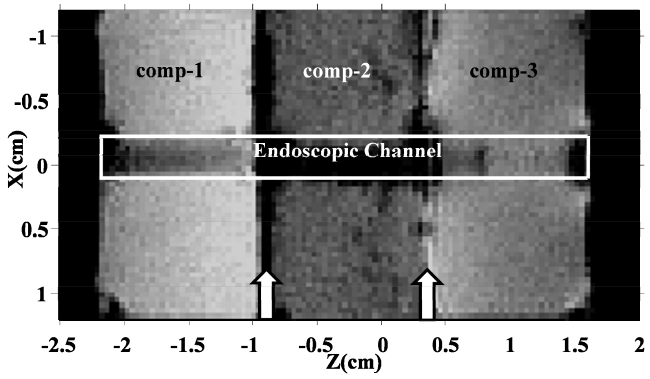

Figure 3. MR image of the 3 compartments phantom collected with the volume RF coil. The vertical arrows point to the boundaries. Scanning is performed in the endoscopic channel. Notable are the chemical shift artifacts due to different species.

(asymmetric truncated quadratic function, threshold: 0.02, 10th order, refer to [9]), and frequency alignment [10]. Beyond the use of dark spectra that were subtracted during data collection, the optical spectra were not subjected to any other processing.

III. Results and Discussion

Table 1 summarizes the results from the MR-compatibility studies (reporting mean SNR ± standard deviation (std), n = 30) for the four operational conditions of the combined motor and encoder assembly. The data in the table illustrate that there are no significant effects on the image or spectral SNR between the states of powered and unpowered, idling and running, of the motor or the optical encoder.

Fig.4 presents results from an experiment that scanned a phantom region along the Z-axis of the MR scanner, transversing the three compartments from position Z = - 1.77 cm to Z = 1.43 cm. Panels (a) and (b) show the LIF and MRS, respectively, illustrating that each compartment exhibits characteristic optical and MR spectral features (simulating scanning tissue with different properties). To appreciate the spatial aspect of the scanning, the LIF and MR spectra were ordered by the co-registration software module based on the exact position at which they were collected along the Z-axis (calculated on-the-fly from the initial registration and the encoder data, and adjusted for the distance between the LIF and MR coil, as shown in Fig. 2). Those data were then presented as spectro-spatial contour plots shown in Figs 4(c) and 4(d). It is noted that for clarity, the ^{1}H spectral width depicted does not include the water signal at 4.9 ppm.

TABLE I. SNR of MR Spectra and Images at various motor and encoder status

Motor Status	*Encoder Status*	*Spectra*	*Images*
unpowered	unpowered	12023±487	72.96±2.79
unpowered	powered	11956±570	77.68±3.80
powered (idle)	powered	12294±530	73.34±2.80
powered (running)	powered	12188±648	73.00±2.81

Both LIF and MR spectro-spatial plots clearly show the two boundaries between the three compartments as manifested by the corresponding resonances. Reflecting the composition of the compartments, the LIF spectra show fluorescein in the comp-1, Rhodamine-B and fluorescein in comp-3, and lack of any fluorophores in the comp-2. Likewise, the spectro-spatial MRS plots exhibit identical patterns: comp-1 has only water signal (at 4.9 ppm not shown), comp-2 has oil signal (-CH_2- resonance at 1.4 ppm), and comp-3 has choline methyl signal (resonance at 3.3 ppm). The two boundaries between compartments were calculated from the MR images to be at Z= -9.2 and 3.3 mm, from LIF spectro-spatial plot at Z=-8.8 and 3.6 mm and from MRS at -8.2 and 3.7 mm, demonstrating the accuracy of co-registration (considering that the scanning resolution is 0.5 mm).

The use of such methodology for localized and co-registered multimodality sensing with MR and optical sensors has potential impact in improving diagnosis *in situ* as well as in

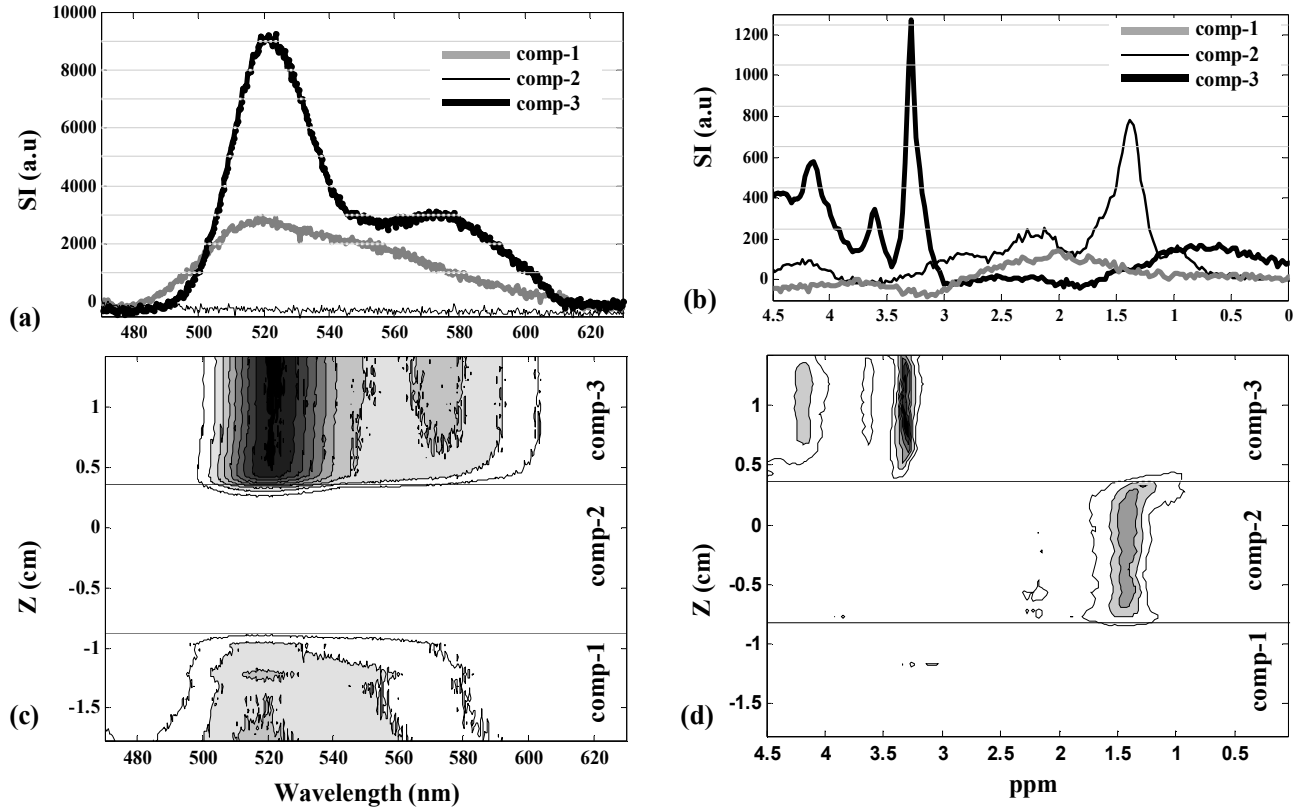

Figure 2. Characteristic **(a)** LIF and **(b)** MR spectra from the center of each compartment. (c, d) Contour plots of stacked **(c)** LIF and **(d)** MR spectra collected along the Z-axis of the MR scanner. Horizontal lines in (c), (d) delineate the boundaries of the compartments. Contour levels in (c) and (d) correspond to the horizontal lines in (a) and (b).

performing basic research in vivo, for instance by co-registered detection of tumor margins and comprehensive diagnosis of pathology.

Although to the best of our knowledge this is the first work that demonstrates multi-modal MR and trans-needle MRS/LIF imaging with automated manipulator positioning, it has certain experimental limitations. Scanning was performed only along the Z-axis of the MR scanner due to the space limit (28 cm clear bore). In a wider-bore clinical scanner, the multi-sensor can be aligned along a wide range of orientations as long as the B_1 rotating field from the RF coil is perpendicular to the main B_O field. Also, while this current work is a suitable proof-of-concept study, *in vivo* studies are needed and planned for the future. The main challenge for *in situ* studies is manufacturing of suitable needles (since an NMR tube is obviously not appropriate for *in vivo* studies). We are also pursuing forward-looking (axial) probes that do not have this limitation, and can be operated clinically in the same way as a standard clinical confocal endoscope, i.e. by placement at the distal end of the scanned area and then being pulled back [11].

IV. CONCLUSIONS

This work describes a novel enabling technology and methodology to perform multi-modality imaging that links multiple modalities (LIF and MRS) and interrogates tissue with locally-deployed sensors to a guiding modality (MRI) that can assess morphology at the macroscopic level. The link is a computer-controlled manipulator that allows the inherent co-registration of the three modalities (LIF, MRS, and MRI) at the level of data collection to the inherent coordinate system of the MR scanner. Experimental studies on multi-compartment phantoms generated one-dimensional spatial distributions of MR and optically distinct entities that demonstrated spatial matching of the three modalities. These data also illustrate the potential of such a method for translating multi-modality scanning and fusion to *in situ* clinical practice. Although our proof-of-concept studies were performed on phantoms, the design criteria, such as the size of the probe and the operational procedures, were selected and developed considering the safety and feasibility for clinical use.

ACKNOWLEDGMENTS

This work was supported by the National Science Foundation (NSF) award CNS-0932272. All opinions, findings, conclusions or recommendations expressed in this work are those of the authors and do not necessarily reflect the views of our sponsors.

REFERENCES

[1] Blasberg, R.G.: Molecular imaging and cancer. Mol Cancer Ther, vol. 2, 335-343 (2003)

[2] Wang, T.D., Van Dam, J.: Optical biopsy: a new frontier in endoscopic detection and diagnosis. Clin Gastroenterol and Hepatol, vol. 2, 744-753 (2004)

[3] Qiu, B., Gao, F., Karmarkar, P., Atalar, E., Yang, X.: Intracoronary MR imaging using a 0.014-inch MR imaging-guidewire: toward MRI-guided coronary interventions. J. Magn. Reson. Imag. 28, 515-518 (2008)

[4] Quick, H.H., Serfaty, J.M., Pannu, H.K., Genadry, R., Yeung, C.J., Atalar, E.: Endourethral MRI. Magn. Reson. Med. 45, 138-146 (2001)

[5] Yang, H.C., Yin, J., Hu, C., Cannata, J., Zhou, Q., Zhang, J., Chen, Z., Shung, K.K.: A dual-modality probe utilizing intravascular ultrasound and optical coherence tomography for intravascular imaging applications. IEEE Trans Ultrason Ferroelectr Freq Control, vol. 57, 2839-2843 (2010)

[6] Sonmez, A.E., Ozcan, A., Spees, W.M., Tsekos, N.V.: Robot-facilitated scanning and co-registration of multi-modal and multi-level sensing: Demonstration with magnetic resonance imaging and spectroscopy. Robotics and Automation, IEEE Int. Conf. on, pp. 1133-1138. (2011)

[7] http://omlc.ogi.edu/spectra/PhotochemCAD/html/rhodamineB.html

[8] Chen, L., Weng, Z., Goh, L.Y., Garland, M.: An efficient algorithm for automatic phase correction of NMR spectra based on entropy minimization. J Magn Reson, vol. 158, 164-168 (2002)

[9] Mazet, V., Carteret, C., Brie, D., Idier, J., Humbert, B.: Background removal from spectra by designing and minimising a non-quadratic cost function. Chemometr. Intell. Lab., vol. 76, 121-133 (2005)

[10] Savorani, F., Tomasi, G., Engelsen, S.B.: icoshift: A versatile tool for the rapid alignment of 1D NMR spectra. J Magn Reson, vol. 202, 190-202 (2010)

[11] Sung, K.B., Liang, C., Descour, M., Collier, T., Follen, M., Richards-Kortum, R.: Fiber-optic confocal reflectance microscope with miniature objective for in vivo imaging of human tissues. IEEE Trans Biomed Eng, vol. 49, 1168-1172 (2002)